Pakistan J. Zool., pp 1-8, 2022. **DOI**: https://dx.doi.org/10.17582/journal.pjz/20211107091103

Protective Mechanism of Velvet Antler Polypeptide on Myocardial Ischemia-Reperfusion Injury in Rats

Ying Chen[1], Chao-Zheng Li[2], Zhun Yu[3], Jia Zhou[4], Yan Xu[4], Zhe Lin[4], He Lin[4]* and Xiao-Wei Huang[4]*

[1]Department of Cardiology, the Affiliated Hospital of Changchun University of Chinese Medicine, Changchun 130021, China
[2]College of Chinese Medicine, Changchun University of Chinese Medicine, Changchun 130117, China
[3]Department of Cardiology, The Third Affiliated Hospital of Changchun University of Chinese Medicine, Changchun 130117, China
[4]School of Pharmacy, Changchun University of Chinese Medicine, Changchun 130117, China

ABSTRACT

Velvet antler polypeptide (VAP) is the active compounds of velvet antler, an animal derived traditional Chinese medicine. In this work, the myocardial ischemia-reperfusion injury (MIRI) model was established to investigate the protective mechanism of VAP on MIRI in rats. Total 90 male Sprague Dawley (SD) rats were divided into the control, model (MIRI), positive (Diltiazem, DLZ, 20 mg/kg), VAP high, medium, low dose (VAP 300, 200, and 100 mg/kg) groups. After 21 days of intragastric administration, the electrocardiogram (ECG) changes in each group were detected. The activities of lactate dehydrogenase (LDH) and creatine kinase-MB (CK-MB) isoenzymes in serum, and superoxide dismutase (SOD), malondialdehyde (MDA), glutathione peroxidase (GSH-Px) and catalase (CAT) in myocardial tissue were detected by ELISA. Hematoxylin and eosin (HandE) staining was used to detect the histological changes of rat myocardium. Western blotting (WB) was used to detect the protein expression levels of nuclear factor erythroid 2-related factor 2 (Nrf2), heme oxygenase-1 (HO-1), and NADH quinone oxidoreductase 1 (NQO1) in rat myocardial tissue. In the results, ECG showed that the MIRI model was successfully established; VAP can significantly reduce the activities of LDH, CK-MB in serum of rats, increase the activities of SOD, GSH-Px, CAT in myocardial tissue, reduce the activity of MDA in myocardial tissue, reduce interstitial edema and inflammatory infiltration, and improve the structural damage of rat myocardial tissue. The expression levels of HO-1, NQO1 and Nrf2 protein in rat myocardial tissue were up-regulated. In conclusion, VAP can improve the structural damage of rat myocardial tissue, improve the antioxidant activity of myocardial, and reduce oxidative stress injury. The relevant mechanism may be related to the regulation of Nrf2/ARE signaling pathway in rat myocardial tissue by VAP.

Article Information
Received 07 November 2021
Revised 20 October 2022
Accepted 14 September 2022
Available online10 January 2023 (early access)

Authors' Contribution
Conceptualization and Methodology: YC, HL. Data curation: ZY. Formal analysis: YC, C-ZL, ZY. Investigation: YC, YX. Software, validation: ZL. Writing-original draft: YC, JZ. Funding acquisition, project administration: HL, X-WH. Writing-review and editing: C-ZL, X-WH. All authors have read and agreed to the published version of the manuscript.

Key words
VAP, Myocardial ischemia reperfusion, Nrf2/ARE signaling pathway, Oxidative stress

INTRODUCTION

Plaque deposition (atherosclerosis) in the coronary artery will lead to partial or complete blockage which blocks the blood supply to the myocardium and reduces the blood flow to the heart, resulting in myocardial ischemia. When the plaque ruptures, it may lead to acute myocardial infarction (AMI), commonly known as heart attack, which will result in instantaneous myocardial ischemia and hypoxia, and directly lead to cell and tissue necrosis. To dredge blood vessels and thrombolysis in clinical will cause further damage to the heart, that is, myocardial ischemia-reperfusion injury (MIRI) (Jennings *et al*., 1960). MIRI is commonly accompanied by inflammatory reaction, leading to reversible and irreversible damage to tissue vitality and organ function. It can further induce myocardial death (Li *et al*., 2020). Therefore, further research on MIRI to minimize its damage is of great significance.

MIRI is reported to be associated with reactive oxygen species (ROS) in body, the production of oxygen free

* Corresponding author: linhe@ccucm.edu.cn, 15948000740@163.com
0030-9923/2022/0001-0001 $ 9.00/0

radicals (Cadenas, 2018), overload of calcium ion (Chang *et al*., 2019), white blood cell inflammation and the lack of high energy phosphoric acid compounds. Oxidative stress is reported to be one of the mechanisms involved in MIRI (Yang *et al*., 2021; Unal *et al*., 2017). Myocardial ischemia will cause a series of traumatic changes in myocardial cell ultrastructure, energy metabolism, cardiac function, electrophysiology, etc., and the damage to tissues and organs will be aggravated, leading to multiple organ failure (Zeng *et al*., 2018). Normally, lactate dehydrogenase (LDH) and creatine kinase-MB (CK-MB) exist in myocardial cells, the myocardial injury will lead to the increase of serum CK-MB and LDH due to the change of permeability. Therefore, they are commonly considered as early diagnostic indicators of AMI (Jiang *et al*., 2017; Herr *et al*., 2020), detecting the activity of LDH and CK-MB in serum can indirectly reflect the degree of myocardial damage (Lu *et al*., 2019). Studies have shown that by increasing the activities of superoxide dismutase (SOD), catalase (CAT), glutathione peroxidase (GSH-Px) and reducing the activity of malondialdehyde (MDA), the oxidative stress damage caused by myocardial ischemia-reperfusion can be suppressed (Tsikas, 2017; Shi *et al*., 2017).

Velvet antler is an animal origin traditional Chinese medicine that from the cartilaginous antler in the precalcified growth stage of the Cervidae family (Bao *et al*., 2018; Qi *et al*., 2020; Zhai *et al*., 2022). China is the region with the most abundant antler resources, and New Zealand is considered to be the largest antler producer in the world. Its main active ingredient extract, velvet antler polypeptide (VAP), has a variety of functions, such as anti-inflammatory, promoting tissue wound healing, improving antioxidant capacity, enhancing immunity, antiviral pharmacological effects, etc. (Bai *et al*., 2017). Studies have shown that VAP had significant protective effects on acute ischemic myocardial injury in rats by anti-oxidation and anti-lipid peroxidation (Chen *et al*., 2009). However, there is lack of further research on the effect of VAP on MIRI and its mechanism.

In this study, MIRI rat model was established, VAP was intragastric administration to observe the effects of VAP on MIRI rats. This study aims to preliminary reveal the mechanism of VAP on MIRI, and provide a theoretical basis for the development and utilization of VAP.

MATERIALS AND METHODS

Materials and animals

VAP was prepared by the School of Pharmacy, Changchun University of Chinese Medicine (Xu *et al*., 2020). The purity of VAP was about 28.7 g velvet antler containing 1.0 g VAP. The detailed reagents and materials were shown in Supplemantary Table S1. Total 90 male SD rats were adaptively fed at 24±1 °C, 12 h light /12 h dark, with normal diet and water for 7 days before the experiment.

Experimental groups and preparation of MIRI model

After that, 90 rats were randomly divided into 6 groups (15 rats per group): The control (Sham operation), model (MIRI), positive (DLZ, Diltiazem 20 mg/kg), VAP high (VAP 300 mg/kg), medium (VAP 200 mg/kg) and low (VAP 100 mg/kg) dosage groups, marked as MIRI + VAPH, MIRI + VAPM, MIRI + VAPL, respectively.

The above dosage was administered intragastric for 21 days. 1 h after the last administration, to establish the MIRI model according to previous study (Simpson *et al*., 1988) with slight revision. In brief, 20% urethane (700 mg/kg, intraperitoneal injection) was used for anesthesia, and the limbs were fixed on the supine operating table with a rubber band (Dasagrandhi *et al*., 2018).

ECG observation and data acquisition

The ECG changes were observed using the PowerLab system (AD Instruments, Bella Vista, Australia) according to related study (Lin *et al*., 2019). Briefly, for each group of the rats, the skin from neck and chest was removed and the trachea was separated. The animal ventilator was connected for endotracheal intubation, with respiration rate of 60-80 times /min and ventilation rate of 20 mL/kg. The thoracic cavity was cut 3 mm from the left edge of the sternum to expose the heart. The needle was inserted at 0.2-0.3 cm from the lower edge of the left auricle, and the pulmonary artery was taken out. A self-made U-shaped rubber tube was inserted and then the descending coronary artery of the left anterior was ligated, and the heart was quickly put back to the chest. After 30 min, the ligature was released to restore the blood supply of the infarcted myocardia and reinfusion of myocardial ischemia was performed. ST segment elevation in the ECG of rats was used as an indicator of myocardial ischemia, and ST segment decrease of 1/2 indicated successful reperfusion.

After 2 h reperfusion, rats were treated and samples were taken from the MIRI, DLZ and VAP groups. For the control group, only thoracotomy was performed and coronary artery was not ligated.

Determination of LDH and CK-MB in serum

After reperfusion, the abdominal cavity of the rats was dissected, and blood sample was collected from the abdominal aorta. The contents of LDH, CK-MB were determined in serum according to the instruction of Elisa kit.

Determination of MDA, SOD, GSH-Px and CAT in myocardial tissue

After reperfusion, 300 mg of myocardial tissue was taken from the ischemic area of the left ventricle immediately. The contents of MDA, SOD, GSH-Px and CAT in myocardial tissue were determined according to the instruction of Elisa kit (Zhao *et al*., 2019).

Hematoxylin and eosin (HandE) staining

After anesthesia, rats in each group were sacrificed, the myocardial tissue was cut off, washed with normal saline, and then placed in 4% paraformaldehyde fixation solution for later use. During the detection, the myocardial tissue was dehydrated, embedded and sectioned into paraffin sections. After staining with H and E, an optical microscope was used to observe the changes in tissue structure (Li *et al*., 2019).

Western blot analysis

The myocardial tissues of rats in each group were taken out and placed in a centrifuge tube. The lysate was added to ice homogenate, the supernatant was obtained after centrifugation, and put at -80°C for later use. The protein concentration of myocardial tissue in each group was calculated by bicinchoninic acid (BCA) assay (Bocian *et al*., 2020). The solution volume was calculated according to the sample concentration, and the protein was denatured by boiling after adding the sample buffer. Polyacrylamide gel was prepared and the denatured protein sample was added. Then, electrophoresis was performed at 90 V for 10 min, then it was performed again at 110 V for 100 min.

After electrophoresis, the gel was removed and the membrane was transferred for 30 min at 200 mA under ice bath. The polyvinylidene fluoride (PVDF) membrane was taken out and sealed in the blocking solution at 4 °C overnight. Then the blocking solution was discarded, and the primary antibody diluent was added and incubated at room temperature for 1 h. After that, the secondary antibody diluent was blocked for 1 h. Then, the luminescence development and gel imaging analysis were performed, β-actin was used as internal standard protein to calculate the expression level of the target protein (Li *et al*., 2019; Sui *et al*., 2021).

Statistical analysis

SPSS 21.0 software (SPSS Inc. Chicago, IL, USA) was used for data processing, and the measurement data were expressed as mean ± standard error. Statistical significance was defined as $p < 0.05$ and $p < 0.01$.

RESULTS

ECG results of each group

ECG was synchronized and recorded by PowerLab. Except for the control group, ST-segment elevation or increased and widened QRS wave could be seen after ligation of the anterior descending branch of the left coronary artery in other groups, and ST-segment recovery was observed after reperfusion, suggesting that the rat MIRI model was successfully established (Fig. 1). The results of ECG showed that the ST segment of the ECG of rats was immediately elevated after the ligation of coronary arteries, and the ST segment decreased by 1/2 after the ligation line was loosened, indicating that the modeling was successful.

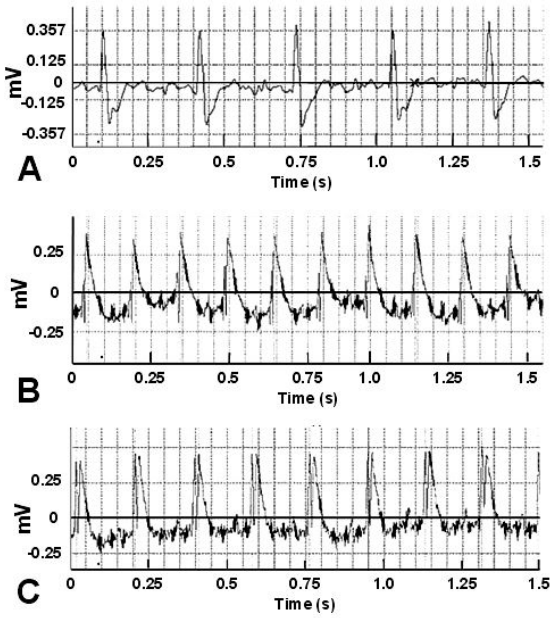

Fig. 1. ECG changes of rats under treatment in each group. A, normal rats; B, ligation ischemia; C, reperfusion 30 min after ligation ischemia.

Changes of LDH, CK-MB Contents in serum

Compared to the control group, the activities of serum myocardial enzymes LDH and CK-MB in MIRI group were remarkably increased ($p<0.01$) (Fig. 2); compared to the MIRI group, the activities of LDH and CK-MB of 300, 200, and 100 mg/kg rats in MIRI + VAP group and DLZ group were remarkably decreased ($p<0.01$) (Fig. 2).

Changes of MDA, SOD, GSH-Px and CAT Contents in myocardial tissue

MDA, SOD, GSH-Px and CAT contents in myocardial tissue were measured. The results showed that,

compared with control group, MDA level in MIRI group was remarkably increased ($p<0.01$) (Fig. 3A), while SOD, GSH-Px, CAT levels were significantly decreased ($p<0.05$, $p<0.01$) (Fig. 3B, C). Compared with the MIRI group, the MDA level in the myocardial tissues in DLZ group and all MIRI + VAP groups were significant decreased ($p<0.01$, $p<0.05$) (Fig. 3A), while the levels of SOD, GSH-Px and CAT were remarkably increased ($p<0.01$, $p<0.05$) (Fig. 3B, C).

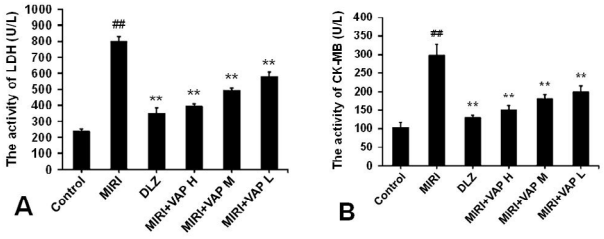

Fig. 2. LDH (A) and CK-MB (B) activities in serum of each group.
Note: ## $p<0.01$, compared with control group; ** $p<0.01$, compared with MIRI group.

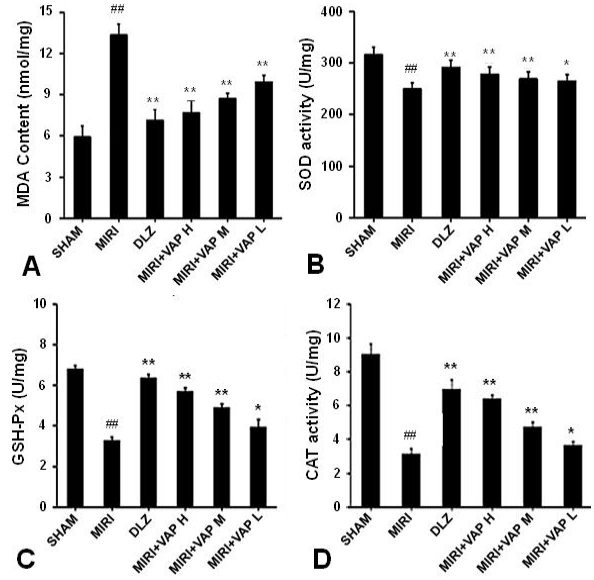

Fig. 3. MDA (A), SOD (B), GSH-Px (C) and CAT (D) activities in myocardial tissue.
Note: Compared with the control group, # $p<0.05$, ## $p<0.01$; Compared with MIRI group,* $p<0.05$, ** $p<0.01$.

The histological changes of myocardial tissue

It can be seen from Figure 4, the myocardial cells in the control group were orderly arranged, with complete cell structure, no intercellular edema, no inflammatory infiltration, and no degeneration and necrosis of cells. In the MIRI group, the myocardial fibers were disordered, the cell tissues were denaturated and necrotic, the interstitial edema was obvious, and the myocardial tissues were infiltrated by a large number of inflammatory cells.

In the positive DLZ group and the VAP groups, the damage of myocardial structure was significantly reduced, a small amount of cell degeneration and necrosis, interstitial edema was reduced, and a small amount of inflammatory cell infiltration was observed, especially in the DLZ group and MIRI + VAP-H group (Fig. 4).

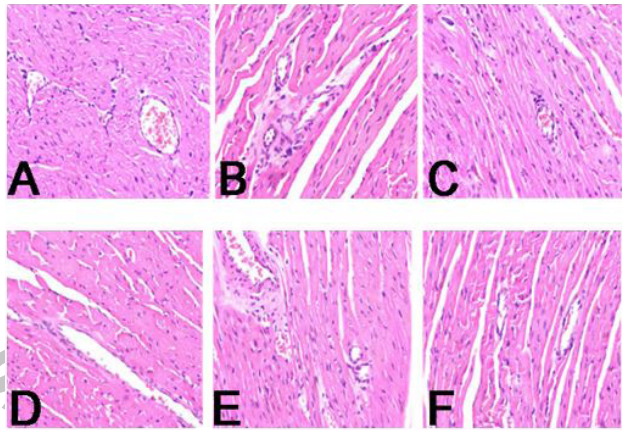

Fig. 4. H and E staining of myocardial tissue in each group (×300). A, Control group; B, MIRI group; C, DLZ group; D, MIRI + VAP-H group; E, MIRI + VAP-M group; F, MIRI + VAP-L group.

The expression levels of Nrf2, HO-1, and NQO1 in myocardial tissue

The gray scale densitometric analyses were conducted using β-actin as an internal reference (Fig. 5). The results showed that, compared with the control group, the difference of Nrf2 protein expression in the cytoplasm of MIRI group was not obvious (Fig. 5A, B). The expression level in the nucleus was remarkably increased ($p<0.01$) (Fig. 5D). Compared to the MIRI group, the difference of Nrf2 protein expression in the cytoplasm of administration group was not obvious (Fig. 5A, B), but the Nrf2 protein expression level in the nucleus was increased ($p<0.01$) (Fig. 5D). Compared with the control group, the protein expression levels of HO-1 and NQO1 in MIRI group were increased ($p<0.01$) (Fig. 5A, C, E). Compared to MIRI group, the protein expressions of HO-1 and NQO1 in DLZ group and VAP administration groups were increased ($p<0.01$, $p<0.05$) (Fig. 5A, C, E). The protein expression levels of HO-1 and NQO1 in DLZ group, MIRI + VAP-H group and MIRI + VAP-M group were more significant than those in other groups ($p<0.01$) (Fig. 5A, C, E). This

suggested that VAP could promote the Nrf2/ARE signaling pathway in MIRI rats.

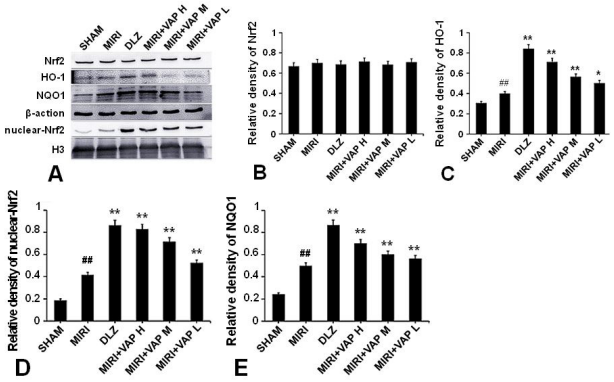

Fig. 5. Effects of VAP on the expression of Nrf2 (A, B, D), HO-1 (A, C), NQO1 (A, E) in MIRI rats by Western blotting.
Note: Compared with Control group, $^{\#\#}$ $p<0.01$; Compared with MIRI group, * $p<0.05$, ** $p<0.01$.

DISCUSSION

The overall research route of this study is shown in Supplementary Figure S1. Generally, LDH, CK-MB exist in myocardial cells, while less in serum. However, when myocardial injury occurs, resulting in the cell permeability increases, thus the content of LDH, CK-MB in serum increases (Hu *et al*., 2017). Therefore, the detection of LDH, CK-MB can be used as indicators to reflect the degree of myocardial cell injury (Cheng *et al*., 2018). The results of this study showed that, the activities of LDH, CK-MB in serum of rats administered with VAP were significantly decreased, suggesting that VAP can significantly reduce the injury of myocardial cells in ischemia reperfusion injury.

Oxidative stress is one of the main factors causing myocardial cell injury and even death during ischemia-reperfusion (Chen *et al*., 2017). SOD and CAT belong to enzymatic antioxidants, while GSH-PX belongs to non-enzymatic antioxidants, both of which can scavenge ROS *in vivo* (Wang *et al*., 2018). MDA is one of the important products of lipid peroxidation in cell membrane, the increase of MDA concentration will cause serious damage to cell membrane. Therefore, the change of MDA content can be used as an indicator of the degree of lipid peroxidation of cell membrane (Tsikas, 2017; Shi *et al*., 2017). The results of this study showed that VAP at different concentrations could reduce the level of MDA and increase the levels of SOD, CAT and GSH-Px in myocardial cells, suggesting that the anti-oxidative stress effect of VAP was important in its myocardial protection.

Ischemic reperfusion injury leads to disorder, looseness and irregularity of myocardial fibers. In addition, it also shows excessive staining or disappearance of nuclei, rupture of myocardial fibers, massive bleeding, and many inflammatory cells can be seen between myocardial fibers (Zhang *et al*., 2016; Li *et al*., 2017; Chen *et al*., 2019). The results of H and E staining showed that, there were obvious pathologic changes in myocardial tissue of the MIRI group. While in DLZ group and all the VAP groups, the myocardial fiber fracture, myocardial hemorrhage and inflammatory cells between myocardial fibers were decreased, suggesting that VAP could improve the pathological changes of myocardial tissue injury by MIRI.

Nrf2 is a major factor regulating cell redox homeostasis. Therefore, Nrf2/ARE signaling pathway plays an important role in cardiac resistance to reperfusion injury (Bai *et al*., 2017; Lee *et al*., 2017). In this study, the results of Western blotting showed that in DLZ group and all the VAP groups, the expression of Nrf2 in the nucleus was significantly increased (Bellezza *et al*., 2018), while that had no significant effect on the total content of Nrf2, indicating that ischemia-reperfusion injury and VAP treatment could promote Nrf2 phosphorylation and nuclear transfer (Fujiki *et al*., 2019). In addition, the protein expressions of HO-1 and NQO1 increased in VAP groups, indicating that ischemia reperfusion injury has a stress stimulation effect on the protein expression of HO-1 and NQO1 (Lin *et al*., 2020; Li *et al*., 2019). These results suggested that VAP can activate the protein expression level of Nrf2 in myocardial cells and upregulate the protein expression levels of HO-1 and NQO1. The development and utilization of VAP will provide an alternative option in clinic, and will also promote the breeding industry of Cervidae family.

CONCLUSION

In summary, this study found that VAP can improve the structural damage of myocardial tissue in MIRI rats, improve the antioxidant activity of myocardium, and reduce oxidative stress injury. The mechanism may be related to the regulation of Nrf2/ARE signaling pathway in myocardial tissue by VAP. This study provides a new possibility and experimental basis for VAP to be used as a potential drug to prevent and treat MIRI.

Ethical compliance

Research experiments conducted in this article with animals were approved by the Animal Care and Welfare Committee of Changchun University of Chinese Medicine (Approval No.: 2020039) following all guidelines,

regulations, legal, and ethical standards as required for animals.

Funding

This work was supported by Hygiene and Health Technology Innovation Project of Jilin province (No.: 2020J068); Traditional Chinese Medicine Science and Technology Project of Jilin Province (No.: 2020056); Innovation Capability Construction Project of Jilin Provincial Development and Reform Commission (No.: 2021C011) and Jilin Province Education Department Project (No.: JJKH20210975KJ).

Supplementary material

There is supplementary material associated with this article. Access the material online at: https://dx.doi.org/10.17582/journal.pjz/20211107091103

Statement of conflict of interest

The authors have declared no conflict of interest.

REFERENCES

Bai, L.N., Shi, W., Liu, J.P., Zhao, X.P., Zhang, Y., Zhou, Z.G., Hou, W. and Chang, T., 2017. Protective effect of pilose antler peptide on cerebral ischemia/reperfusion (I/R) injury through Nrf-2/OH-1/NF-andkappa B pathway. *Int. J. Biol. Macromol.,* **102**: 741-748. https://doi.org/10.1016/j.ijbiomac.2017.04.091

Bao, N., Yin, Y.G. and Wang, P.P., 2018. An antimicrobial cerebroside from the liposoluble constituent of cervus nippon antler velvet layer. *Pakistan J. Zool.,* **50**: 1747-1751. https://doi.org/10.17582/journal.pjz/2018.50.5.1747.1751

Bellezza, I., Giambanco, I., Minelli, A. and Donato, R., 2018. Nrf2-Keap1 signaling in oxidative and reductive stress. *Biochim. Biophys. Acta Mol. Cell Res.*, **1865**: 721-733. https://doi.org/10.1016/j.bbamcr.2018.02.010

Bocian, A., Sławek, S., Jaromin, M., Hus, K.K., Buczkowicz, J., Łysiak, D., Petrílla, V., Petrillova, M., Legáth, J., 2020. Comparison of methods for measuring protein concentration in venom samples. *Animals*, **10**: 448. https://doi.org/10.3390/ani10030448

Cadenas, S., 2018. ROS and redox signaling in myocardial ischemia reperfusion injury and cardioprotection. *Free Radical Biol. Med.*, **117**: 76-89. https://doi.org/10.1016/j.freeradbiomed.2018.01.024

Chang, J.C., Lien, C.F., Lee, W.S., Chang, H.R., Hsu, Y.C., Luo, Y.P., Jeng, J.R., Hsieh, J.C. and Yang, K.T., 2019. Intermittent hypoxia prevents myocardial mitochondrial Ca^{2+} overload and cell death during ischemia/reperfusion: the role of reactive oxygen species. *Cells*, **8**: 564. https://doi.org/10.3390/cells8060564

Chen, C., Lu, W., Wu, G., Lv, L., Chen, W., Huang, L, Wu, X., Xu, N. and Wu, Y., 2017. Cardioprotective effects of combined therapy with diltiazem and superoxide dismutase on myocardial ischemia-reperfusion injury in rats. *Life Sci.,* **183**: 50-59. https://doi.org/10.1016/j.lfs.2017.06.024

Chen, C.L., Wang, S.C. and Liu, P., 2019. Deferoxamine enhanced mitochondrial iron accumulation and promoted cell migration in triple-negative MDA-MB-231 breast cancer cells via a ROS-dependent mechanism. *Int. J. mol. Sci.*, **20**: 4952. https://doi.org/10.3390/ijms20194952

Chen, X.G., Wang, Y., Wu, Y., Wang, L.P. and Li, W., 2009. Protective effects of peptides from velvet antler of *Cervus nippon* on acute ischemic myocardial injury in rats. *China J. Chin. Mater. Med.*, **34**: 1971-1974.

Cheng, Y., Tan, J., Li, H., Kong, X., Liu, Y., Guo, R., Li, G., Yang, B. and Pei, M., 2018. Cardioprotective effects of total flavonoids from Jinhe Yangxin prescription by activating the PI3K/Akt signaling pathway in myocardial ischemia injury. *Biomed. Pharmacother.*, **98**: 308-317. https://doi.org/10.1016/j.biopha.2017.12.052

Dasagrandhi, D., Kamalabai, R.A.S., Muthuswamy, A., Lennox, A.M., Jayavelu, T., Devanathan, V. and Swaminathan, J.K., 2018. Ischemia/reperfusion injury in male guinea pigs: An efficient model to investigate myocardial damage in cardiovascular complications. *Biomed. Pharmacother.*, **99**: 469-479. https://doi.org/10.1016/j.biopha.2018.01.087

Fujiki, T., Ando, F., Murakami, K., Isobe, K., Mori, T., Susa, K., Nomura, N., Sohara, E., Rai, T. and Uchida, S., 2019. Tolvaptan activates the Nrf2/HO-1 antioxidant pathway through PERK phosphorylation. *Sci. Rep.*, **9**: 9245(1)-9245(10). https://doi.org/10.1038/s41598-019-45539-8

Herr, D.J., Singh, T. and Dhammu, T., 2020. Regulation of metabolism by mitochondrial enzyme acetylation in cardiac ischemia-reperfusion injury. *Biochim. biophys. Acta, Mol. Basis Dis.,* **1866**: 1-8. https://doi.org/10.1016/j.bbadis.2020.165728

Hu, L., Cai, N. and Jia, H., 2017. Pterostilbene attenuates myocardial ischemia-reperfusion injury via the phosphatidylinositol 3'-kinase-protein kinase B signaling pathway. *Exp. Ther. Med.*, **14**: 5509-5514.

Jennings, R.B., Sommers, H.M., Smyth, G.A., Flack,

H.A. and Linn, H., 1960. Myocardial necrosis induced by temporary occlusion of a coronary artery in the dog. *Arch. Pathol.*, 70: 68-78.

Jiang, M., Wang, Q., Chen, J., Wang, Y., Fan, G. and Zhu, Y., 2017. Comparative metabonomics of Wenxin Keli and Verapamil reveals differential roles of gluconeogenesis and fatty acid β-oxidation in myocardial injury protection. *Sci. Rep.*, 7: 8739. https://doi.org/10.1038/s41598-017-09547-w

Lee, Y.J., Beak, S.Y., Choi, I. and Sung, J.S., 2017. Quercetin and its metabolites protect hepatocytes against ethanol-induced oxidative stress by activation of Nrf2 and AP-1. *Food Sci. Biotechnol.*, **27**: 809-817. https://doi.org/10.1007/s10068-017-0287-8

Li, H.T., Liu, C.G., Bao, M.H., Liu, W.J., Nie, Y., Lian, H. and Hu, S.S., 2020. Optimized Langendorff perfusion system for cardiomyocyte isolation in adult mouse heart. *J. cell. mol. Med.*, **24**: 14619-14625. https://doi.org/10.1111/jcmm.15773

Li, T., Wang, X., Zhang, H., Chen, Z., Zhao, X., Ma, Y. 2019. Histomorphological comparisons and expression patterns of *BOLL* gene in sheep testes at different development stages. *Animals*, **9**: 105. https://doi.org/10.3390/ani9030105

Li, X., Wu, N., Zou, L. and Jia, D., 2017. Protective effect of celastrol on myocardial ischemia-reperfusion injury. *Anatolian J. Cardiol.*, **18**: 384-390. https://doi.org/10.14744/AnatolJCardiol.2017.7866

Li, X.G., Liu, Z.D., Zhang, A., Han, C.H., Shen, A.J., Jiang, L.X., Boothman, D.A., Qiao, J., Wang, Y., Huang, X.M. and Fu, Y.X., 2019. NQO1 targeting prodrug triggers innate sensing to overcome checkpoint blockade resistance. *Nat. Commun.,* **10**: 3251. https://doi.org/10.1038/s41467-019-11238-1

Lin, C.C., Lin, W.N., Cho, R.L., Yang, C.C., Yeh, Y.C., Hsiao, L.D., Tseng, H.C. and Yang, C.M., 2020. Induction of HO-1 by mevastatin mediated via a Nox/ROS-dependent c-Src/PDGFRα/PI3K/Akt/Nrf2/ARE cascade suppresses TNF-α-induced lung inflammation. *J. Clin. Med.*, **9**: 226. https://doi.org/10.3390/jcm9010226

Lin, H.Y., Chou, P.C., Chen, Y.H., Lai, L.S., Chung, T.K., Walzem, R.L., Huang, S.Y. and Chen, S.E., 2019. Dietary supplementation of 25-hydroxycholecalciferol improves livability in broiler breeder hens-amelioration of cardiac pathogenesis and hepatopathology. *Animals*, **9**: 770. https://doi.org/10.3390/ani9100770

Lu, Q.Y., Ma, J.Q., Duan, Y.Y., Sun, Y., Yu, S., Yu, S. H., Li, B. and Zhang, G. M., 2019. Carthamin yellow protects the heart against ischemia/reperfusion injury with reduced reactive oxygen species release and inflammatory response. *J. Cardiovasc. Pharmacol.,* **74**: 228-234. https://doi.org/10.1097/FJC.0000000000000710

Qi, L., Li, L., Chen, D.Y., Liu, M.X., Wu, Y. and Hu, W., 2020. Isolation and purification of 18KD protein of sika deer antler plate and its antibacterial activity. *Pakistan J. Zool.,* **52**: 7-14. https://doi.org/10.17582/journal.pjz/2020.52.1.7.14

Shi, C., Chen, X., Liu, Z., Meng, R., Zhao, X., Liu, Z. and Guo, N., 2017. Oleuropein protects L-02 cells against H_2O_2-induced oxidative stress by increasing SOD1, GPx1 and CAT expression. *Biomed. Pharmacother.,* **85**: 740-748. https://doi.org/10.1016/j.biopha.2016.11.092

Simpson, P. J., Fantone, J. C., Mickelson, J. K., Gallagher, K.P. and Lucchesi, B.R., 1988. Identification of a time window for therapy to reduce experimental canine myocardial injury: Suppression of neutrophil activation during 72 hours of reperfusion. *Circ. Res.*, **63**: 1070-1079. https://doi.org/10.1161/01.RES.63.6.1070

Sui, X., Zhou, J., Xu, Y., Wang, Y.C., Lv, G.F., Lin, H., Huang, X.W., Deng, Y., 2021. Biological and molecular evidences for the antitumor potential of EGb 761 in glioma cells in vitro and in vivo. *J. Biobased Mater. Bioenergy*, **15**: 685-692. https://doi.org/10.1166/jbmb.2021.2094

Tsikas, D., 2017. Assessment of lipid peroxidation by measuring malondialdehyde (MDA) and relatives in biological samples: Analytical and biological challenges. *Anal. Biochem.*, **524**: 13-30. https://doi.org/10.1016/j.ab.2016.10.021

Unal, B., Ozcan, F., Tuzcu, H., Kırac, E., Elpek, G.O. and Aslan, M., 2017. Inhibition of neutral sphingomyelinase decreases elevated levels of nitrative and oxidative stress markers in liver ischemia-reperfusion injury. *Redox Rep.*, **22**: 147-159. https://doi.org/10.1080/13510002.2016.1162431

Wang, Y., Branicky, R., Noë, A. and Hekimi, S., 2018. Superoxide dismutases: Dual roles in controlling ROS damage and regulating ROS signaling. *J. Cell Biol.*, **217**: 1915-1928. https://doi.org/10.1083/jcb.201708007

Xu, Y., Zhou, J., Lv, G.F., Liu, Y.X., Zhao, X.T., Li, X., Ye, D.D., Qu, X.B. and Huang, X.W., 2020. Effect of pilose antler peptide on doxorubicin-induced H9c2 cells injury via TGF-β/Smad/ERK signaling pathway. *Pakistan J. Zool.,* **52**: 1787-1793. https://doi.org/10.17582/journal.pjz/20200218020203

Yang, W.C., Cao, H.L., Wang, Y.Z., Li, T.T., Hu, H.Y.,

Wan Q. and Li W.Z., 2021. Inhibition of nitric oxide synthase aggravates brain injury in diabetic rats with traumatic brain injury. *Neural Regener. Res.*, 16: 1574-1581. https://doi.org/10.4103/1673-5374.303035

Zeng, C., Jiang, W., Yang, X., He, C., Wang, W. and Xing, J., 2018. Pretreatment with total flavonoid extract from dracocephalum moldavica *L. attenuates* ischemia reperfusion-induced apoptosis. *Sci. Rep.*, **8**: 17491. https://doi.org/10.1038/s41598-018-35726-4

Zhang, L., Ding, W.Y., Wang, Z.H., Tang, M.X., Wang, F., Li, Y., Zhong, M., Zhang, Y. and Zhang, W., 2016. Early administration of trimetazidine attenuates diabetic cardiomyopathy in rats by alleviating fibrosis, reducing apoptosis and enhancing autophagy. *J. Transl. Med.,* **14**: 109. https://doi.org/10.1186/s12967-016-0849-1

Zhai, J.C., Wang, S.N., Wang, Q.H. and Xia, Y.L., 2022. Differential DNA methylation of growth factors in antlers of sika deer and reindeer. *Pakistan J. Zool., Early Access*, https://doi.org/10.17582/journal.pjz/20190718030701

Zhao, Y., Niu, Y., He, J., Zhang, L., Wang, C., Wang, T., 2019. Dietary dihydroartemisinin supplementation attenuates hepatic oxidative damage of weaned piglets with intrauterine growth retardation through the Nrf2/ARE signaling pathway. *Animals*, **9**: 1144. https://doi.org/10.3390/ani9121144

Pakistan J. Zool., pp 1-8, 2022. **DOI**: https://dx.doi.org/10.17582/journal.pjz/20211107091103

Supplementary Material

Protective Mechanism of Velvet Antler Polypeptide on Myocardial Ischemia-Reperfusion Injury in Rats

Ying Chen[1], Chao-Zheng Li[2], Zhun Yu[3], Jia Zhou[4], Yan Xu[4], Zhe Lin[4], He Lin[4]* and Xiao-Wei Huang[4]*

[1]Department of Cardiology, the Affiliated Hospital of Changchun University of Chinese Medicine, Changchun 130021, China
[2]College of Chinese Medicine, Changchun University of Chinese Medicine, Changchun 130117, China
[3]Department of Cardiology, The Third Affiliated Hospital of Changchun University of Chinese Medicine, Changchun 130117, China
[4]School of Pharmacy, Changchun University of Chinese Medicine, Changchun 130117, China

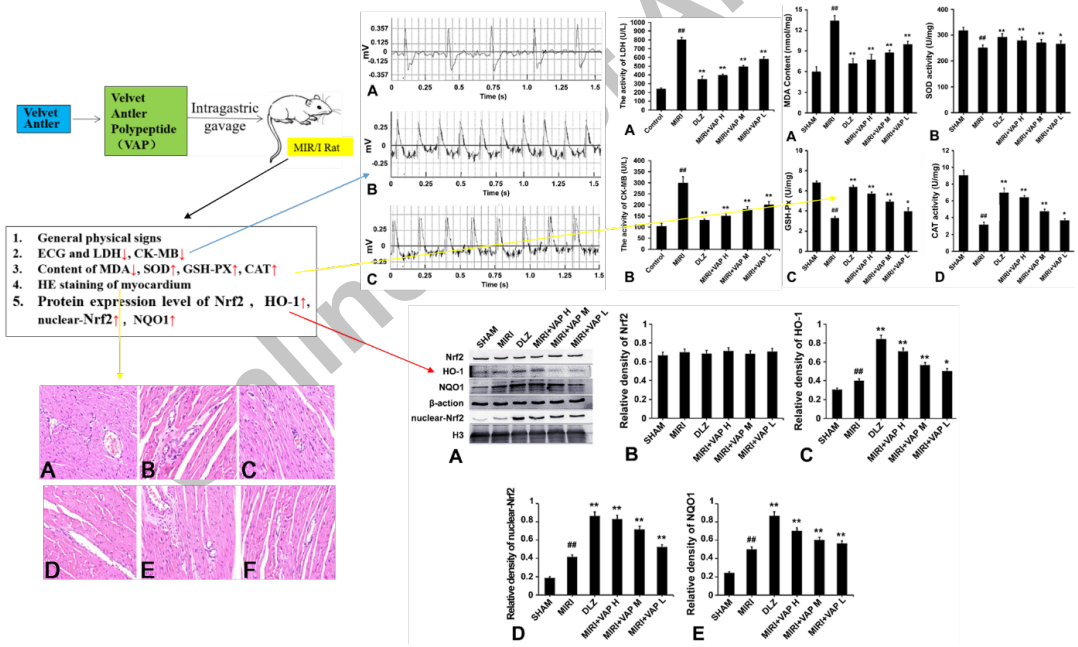

Supplementary Fig. S1. The overall research plan of this paper.

* Corresponding author: linhe@ccucm.edu.cn, 15948000740@163.com
0030-9923/2022/0001-0001 $ 9.00/0

Supplementary Table SI. Main reagents and materials used in this study.

Reagents and materials	Manufacturers
AA mixed standard (BWT30103-1-C-1)	Tanmo Quality Testing Technology Co., Ltd, Beijing, China
Hematoxylin Staining Solution (D1120), Eosin Staining Solution (G1120-100)	Solarbio Science and Technology Co., Ltd, Beijing, China
LDH Elisa kit (A020-2-2), SOD Elisa kit (A001-3-2), MDA Elisa kit (A003-1-2), GSH-Px Elisa kit (A005-1-2), CAT Elisa kit (A007-2-1)	Jiancheng Biological Engineering Research Institute, Nanjing, China
Creatine kinase-MB (CK-MB) isoenzymes Elisa kit (MM-0625R2)	Jiangsu Enzymatic Co., Ltd, Taizhou, China
HO-1/HMOX1 Polyclonal Antibody (10701-1-AP), NQO1 Polyclonal Antibody (11451-1-AP), NRF2, NFE2L2 Polyclonal Antibody (16396-1-AP), Beta Actin Monoclonal Antibody (66009-1-Ig), Histone-H3 Polyclonal antibody (17168-1-AP)	Sanying Biology Technology Co., Ltd, Wuhan, China
Anti-Nrf2 (phospho S40) antibody [EP1809Y] (ab76026)	Abcam Trading Co., Ltd, Shanghai, China
Sprague Dawley (SD) rats (male, n=90)	Yisi Experimental Animal Technology Co., LTD. (Chuangchun, China. License No.: SCXK-JI 2018-0007).